

Poly(L-lysine)-g-Poly(ethylene glycol) Layers on Metal Oxide Surfaces: Attachment Mechanism and Effects of Polymer Architecture on Resistance to Protein Adsorption[†]

Gregory L. Kenausis,[‡] Janos Vörös,[‡] Donald L. Elbert,[§] Ningping Huang,[‡] Rolf Hofer,[‡] Laurence Ruiz-Taylor,^{‡,||} Marcus Textor,[‡] Jeffrey A. Hubbell,[§] and Nicholas D. Spencer^{*,‡}

Laboratory for Surface Science and Technology and Institute for Biomedical Engineering, Department of Materials, ETH Zurich, CH-8092 Zurich, Switzerland

Received: September 20, 1999; In Final Form: January 21, 2000

The generation of surfaces and interfaces that are able to withstand protein adsorption is a major challenge in the design of blood-contacting materials for both medical implants and bioaffinity sensors. Poly(ethylene glycol)-derived materials are generally considered to be particularly effective candidates for the fabrication of protein-resistant materials. Most metallic biomaterials are covered by a protective, stable oxide film; converting such oxide surfaces, which are known to strongly interact with proteins, into noninteractive surfaces requires a specific design of the surface/interface architecture. A class of copolymers based on poly(L-lysine)-g-poly(ethylene glycol) (PLL-g-PEG) was found to spontaneously adsorb from aqueous solutions onto several metal oxide surfaces, such as TiO₂, Si_{0.4}Ti_{0.6}O₂, and Nb₂O₅, as measured by the in situ optical waveguide lightmode spectroscopy technique and by ex situ X-ray photoelectron spectroscopy. The resulting adsorbed layers are highly effective in reducing the adsorption both of blood serum and of individual proteins such as fibrinogen, which is known to play a major role in the cascade of events that lead to biomaterial-surface-induced blood coagulation and thrombosis. Adsorbed protein levels as low as <5 ng/cm² could be achieved for an optimized polymer architecture. The modified surfaces are stable to desorption under flow conditions at 37 °C and pH 7.4 in HEPES [4-(2-hydroxyethyl)piperazine-1-ethanesulfonic acid] and PBS (phosphate-buffered saline) buffers. The adsorbed layer of copolymer is thought to form a comblike structure at the surface, with positively charged primary amine groups of the PLL bound to the negatively charged metal oxide surface, while the hydrophilic and uncharged PEG side chains are exposed to the solution phase. Copolymer architecture is an important factor in the resulting protein resistance; it is discussed on the basis of packing-density considerations and the corresponding radii of gyration of the different PEG chain lengths studied. This surface functionalization technology is believed to be of value for use in both the biomaterial and biosensor areas, as the chosen macromolecules are biocompatible and the application is straightforward and cost-effective.

1. Introduction

1.1. General Background. Nonspecific protein adsorption plagues a wide array of biomedical devices, such as catheters, heart valves, and stents, as well as blood-, serum-, or plasma-contacting sensors.¹ Protein adsorption onto the implant surface is the first stage in the series of events that, depending on the type and nature of the adsorbed proteins, may lead to a deleterious response. In the case of blood-contacting devices such as stents and catheters, in particular, protein adsorption is the first step in a cascade of surface processes that induce platelet deposition and thrombus formation. Because metals such as titanium or steel, covered by their related surface oxides, are often applied in blood-contacting devices, a method for reducing protein adsorption on oxides would be an important development in biomaterials technology. Moreover, oxides of transition metals, such as titanium, tantalum, or niobium, are preferred surface coatings for optical waveguides because of their high

optical transparency and high index of refraction. Optical waveguide lightmode spectroscopy (OWLS) is a sensitive detection approach for biomolecule sensing because of its high interfacial sensitivity. In general, a technique for reducing nonspecific adsorption in a consistent manner is required to improve the performance of analyte-specific sensors in terms of both selectivity and sensitivity.

Poly(ethylene glycol) (PEG) has been extensively investigated for use in a wide array of biomedical applications, and immobilization of PEG on surfaces has long been known to decrease protein adsorption. Of the many models proposed to explain this effect, steric stabilization and excluded-volume effects are the most commonly cited.^{2–4} A general approach to the immobilization of PEG on surfaces involves the coupling of PEG to a functional group that has an affinity for the target surface. Processes ranging from chemical surface derivatization with reactively functionalized PEG^{5–7} to adsorption of PEG-containing surfactants such as Pluronics⁸ have been studied extensively. In the latter case, treatment of hydrophobic surfaces with Pluronics resulted in surfaces that were resistant to protein adsorption and platelet adhesion.^{9–11}

Another approach to PEG immobilization involves the grafting of PEG side chains onto a polymer backbone, resulting

[†] Part of the special issue "Gabor Somorjai Festschrift".

* Corresponding author. E-mail: nspencer@surface.mat.ethz.ch. Tel.: +41 1 632 5850. Fax: +41 1 633 10 27.

[‡] Laboratory for Surface Science and Technology.

[§] Institute for Biomedical Engineering.

^{||} Present address: Zyomyx, Inc., 3911 Trust Way, Hayward, CA 94545.

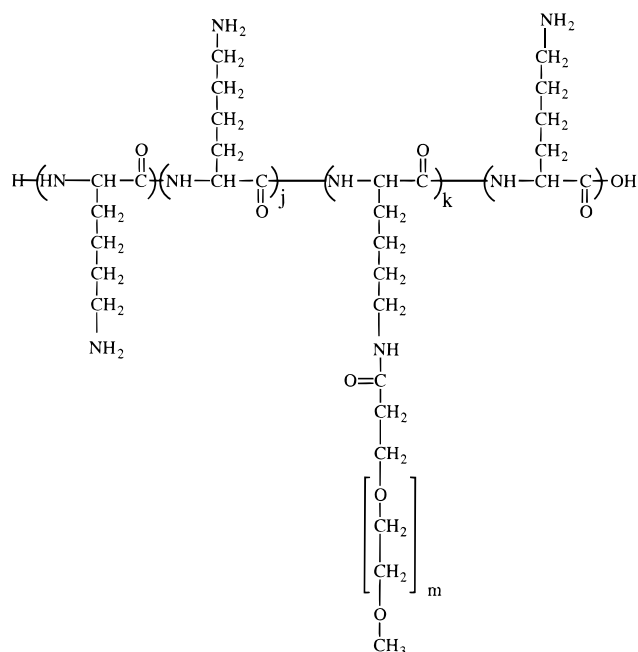


Figure 1. Chemical structure of the poly(L-lysine)-g-poly(ethylene glycol) (PLL-g-PEG) polymer. (See the first paragraph of section 2 for a comprehensive description of the specific structures of the various PLL-g-PEG polymers discussed in this paper.)

in the formation of a comblike structure.^{2,12,13} The adsorption behavior of graft copolymers, in general, has been modeled by several authors^{14–20} and clearly depends on the interaction between the polymer backbone and the target surface.

The aim of the present study was to immobilize PEG on metal oxide surfaces such as silicon dioxide, titanium dioxide, and niobium pentoxide. The adsorption behavior of polyelectrolytes on such metal oxide surfaces has been characterized,^{21–27} and polycations, in particular, were found to form stable adsorbed layers on negatively charged oxides such as silicon dioxide and titanium dioxide.

The polymer system investigated in the present study, poly(L-lysine)-g-poly(ethylene glycol) (PLL-g-PEG), consists of a poly(L-lysine) (PLL) backbone that has been grafted with PEG side chains (see Figure 1).⁵¹ PLL was chosen as the polymer backbone because it is highly cationic at physiological pH and because PLL is a polypeptide with well-understood toxicology.²⁸ Furthermore, graft copolymers of PLL and PEG and similar, related polymers have been evaluated for toxicity, immunogenicity, immunomodulatory potential, pyrogenicity, and biodegradation, largely in the context of drug delivery^{29–33} and tissue adhesion suppression.^{24–27,34}

In the present study, the assembly of an adsorbed layer of the PLL-g-PEG copolymer onto several metal oxide surfaces is shown to be caused by the electrostatic interaction of the positively charged PLL backbone with the negatively charged metal oxide surfaces. This, then, presumably creates a surface-bound comb of PEG. The resultant surfaces have been found to exhibit drastically reduced protein adsorption relative to the untreated metal oxide control surfaces. Because this immobilization relies on electrostatic interactions in an electrolyte, pH and ionic strength are clearly important parameters in determining the extent and stability of such adsorption. Because of its versatility, high sensitivity, and suitability for *in situ* measurements,^{35–38} the optical waveguide lightmode spectroscopy (OWLS) technique was employed, as it is well-suited for the

quantitative determination of copolymer adsorption and stability, as well as inhibition of protein adsorption. Additionally, X-ray photoelectron spectroscopy was used to assess the properties of the adsorbed layer of PLL-g-PEG and its interaction with the underlying metal oxide surface.

1.2. Review of the Surface Adsorption of Graft Copolymers and Polyelectrolytes. An understanding of the ability of adsorbed copolymers to passivate a surface against the adsorption of proteins will rely heavily on previous work concerning the steric stabilization of colloids because of the colloidal nature of individual protein molecules. From studies of polymeric steric stabilization, it is clear that the ability to stabilize a suspension of colloids will depend on the ability to immobilize an otherwise soluble polymer on the colloid surface. This can be achieved through chemical grafting of the polymer, through initiation of polymerization at the colloid surface, or through adsorption. Of these techniques, adsorption is perhaps the simplest means for immobilizing polymer on the colloid surface. Compared with homopolymers and random copolymers, block copolymers will typically be more useful for achieving adsorption and steric stabilization on a surface. Block copolymers of different architectures have been utilized in this regard, such as AB, ABA, BAB, (AB)_n, and A(B)_n (that is, comb graft copolymer), as well as dendrimeric-type structures.³⁹

In aqueous solution, the great majority of surfactants for the dispersion of colloids are not polymers, but rather charged long-chain hydrocarbons, with stability imparted by electrostatic stabilization. However, electrostatic stabilization is not generally feasible for the prevention of protein adsorption onto surfaces, because proteins will generally present a balance of positive and negative residues. Polymeric steric stabilization is much more appropriate, and in aqueous media, this is most often accomplished with nonionic surfactants. These are most often poly(ethylene glycol)s, attached to various hydrophobic components, such as alkyl phenols, alkyl alcohols, fatty acids, and water-insoluble polyalkyl glycols. Because the adsorption of the polymer will generally be irreversible, the thermodynamics and kinetics of adsorption will be important, as these will determine the surface density of poly(ethylene glycol) segments. To achieve efficient steric stabilization, the surface spacing of bound poly(ethylene glycol) units should be less than the radius of gyration of poly(ethylene glycol) in solution.²⁰

An important theoretical result is that, as the polymer chains adsorb onto the surface, the amount of space left for other chains decreases, and thus, an adsorption isotherm will be observed. This is particularly important with block copolymers, because of the large volume of the adsorbing segment and because of the steric effects of the poly(ethylene glycol) segments. A fast adsorption step is observed, followed by slow surface rearrangements that allow the adsorption of more polymer.^{40–42} To achieve efficient protein repulsion, a balance must be found so as to maximize the ratio of the radius of gyration of poly(ethylene glycol) to the distance between attachment sites of the poly(ethylene glycol) segments, while still adsorbing the copolymer to the surface essentially irreversibly.

Numerous examples of these systems have been studied experimentally. Tirrell et al.⁴³ measured the adsorption of AB copolymers of polystyrene and polyvinylpyridine on mica. A wide range of molecular weights was tested, and it was found that, for most samples, about 200 ng/cm² of polymer adsorbed to the surface, and that the buoy segments easily formed “polymer combs”, unless the size of the anchoring segment was too large. The maximum surface density was found with small

TABLE 1: Details of the Synthesis of Different Types of PLL-g-PEG

polymer PLL(<i>x</i>)-g[<i>y</i>]-PEG(<i>z</i>) ^a	PLL	PEG
PLL(375)-g[5.6]-PEG(5)	500 mg in 10 mL of SBB ^b	2.0 g in 2.5 mL of SBB ^b
PLL(20)-g[6.0]-PEG(5)	500 mg in 10 mL of SBB ^b	2.0 g in 2.5 mL of SBB ^b
PLL(20)-g[3.5]-PEG(2)	83.6 mg in 1.05 mL of STBB ^c	215.7 mg of solid
PLL(20)-g[5.5]-PEG(2)	106.8 mg in 1.34 mL of STBB ^c	193.2 mg of solid

^a PLL(*x*)-g[*y*]-PEG(*z*) signifies that the graft copolymer has a PLL backbone of mol wt *x* kDa; a graft ratio, *y*, of lysine-mer/PEG side chain; and PEG side chains of mol wt *z* kDa. ^b SBB is sodium borate buffer (pH 8.5). ^c STBB is sodium tetraborate buffer (pH 8.5).

anchor segments and intermediate-sized buoy segments, as would be expected for a copolymer containing anchor segments with strong binding capabilities.⁴³

The adsorption of polyelectrolytes, in particular, onto surfaces has been reviewed,^{20,44} and it has been found that, in general, the polyelectrolyte will attempt to neutralize any opposite charge present on the surface. Furthermore, the presence of polyelectrolyte loops and tails leads to an overcompensation and a reversal of surface charge. A polyelectrolyte will generally remain very close to the surface, orienting parallel to the surface and producing very thin layers, often less than the radius of gyration of the polymer, with the layer thickness increasing as the concentration of salt is decreased.²⁰ The concentration of salt is important and may aid or hinder adsorption of the polyelectrolyte. An increase in salt concentration decreases interpolyelectrolyte repulsion, leading to enhanced adsorption of the polymer, but also compacts the electric double layer, leading to repulsion and competition for surface ions, which, in turn, lead to desorption of the polymer. The adsorption of polylysine on silica was found to be maximal at 10–100 mM NaCl (physiological NaCl concentration is 150 mM), and the adsorbed amount of the polymer increased almost linearly with an increase in surface charge.⁴⁴ The kinetics of adsorption and desorption of polycations on titanium dioxide and silicon dioxide have also been studied.^{22,23} The initial adsorption was found to be transport-limited, and a maximum in the amount adsorbed was found at a salt concentration of about 100 mM. Desorption of polycations after the polycation solution was replaced with 100 mM NaCl was slow even under flow. However, changing the pH so as to neutralize the charge of the polymer or the surface led to rapid desorption of the polymer.

2. Materials and Methods

For clarity, the following system of abbreviations will be used when referring to the various polymers discussed in this paper: PLL(*x*)-g[*y*]-PEG(*z*) signifies that the graft copolymer has a PLL backbone of molecular weight *x* kDa; a graft ratio, *y*, of lysine-mer/PEG side chain; and PEG side chains of mol wt *z* kDa.

2.1. Synthesis of PLL-g-PEG. Table 1 shows the details of the masses and solvents that were used to synthesize the different polymers according to the following procedure. Poly-L-lysine hydrobromide of mol wt 20 000 or 375 000 (Sigma, St. Louis, MO) was dissolved in 50 mM sodium borate buffer (SBB), pH 8.5. The solution was filter sterilized (0.2- μ m pore-size filter). Monomethoxy PEG-nitrophenyl carbonate, mol wt 5000 (Shearwater Polymers, Huntsville, AL), or *N*-hydroxysuccinimidyl ester of methoxypoly(ethylene glycol) propionic acid, mol wt

2000 (SPA-PEG, Shearwater Polymers Europe, Inc.), was either quickly dissolved with stirring in 2.5 mL of 50 mM SBB, pH 8.5, or taken as a solid and added to the dissolved PLL. The reaction was allowed to proceed for 6 h at room temperature, after which the reaction mixture was dialyzed (Spectra-Por, mol wt cutoff 12 000–14 000; Spectrum, Houston, TX) for 24 h, first against phosphate-buffered saline (PBS; 0.2 g/L KCl, 0.2 g/L KH₂PO₄, 8 g/L NaCl, 1.15 g/L anhydrous Na₂HPO₄, pH 7.4 \pm 0.1, 285 \pm 5% mOsm/kg H₂O) and subsequently against deionized water. The product mixture was freeze-dried and stored at –20 °C under Ar. PLL(375)-g(5.6)-PEG(5): ¹H NMR (D₂O, ppm) 1.35, 1.60, 1.68 (–CH₂–), 2.88 (–CH₂–N–), 3.55 (PEG), 4.20 (–N–CHR–COO–). By NMR, the areas of the lysine side-chain peaks were compared with the area of the PEG peak to determine the graft ratio of the comb copolymer. Graft ratios of the PLL-g-PEG copolymers were also analyzed by aqueous size-exclusion chromatography using refractive index detection (Shodex OHpak column, SB-804HQ, Alltech, Deerfield, IL; Delory & King's carbonate–bicarbonate buffer eluent, 0.2 M anhydrous sodium carbonate and 0.2 M sodium bicarbonate mixed to make pH 10; sample was 1% in eluent buffer). Graft ratios were estimated by comparing the area of the free PEG peak with the area of the PLL-g-PEG peak, assuming that PEG and PLL-g-PEG have identical, linear refractive index increments in this concentration range. Because free mPEG is not removed during dialysis, the amount of PEG coupled to poly(L-lysine) can be calculated. The reported graft ratios were determined by the chromatographic method.

A dendron copolymer (Dendron-5) was prepared according to the following procedure. Monomethoxy PEG of mol wt 20 000 (PEG 20K; Shearwater Polymers, Huntsville, AL) was dried by azeotropic distillation from benzene. The hydroxyl terminus of the PEG was first esterified with Fmoc-Gly. The anhydride of Fmoc-Gly was produced by the reaction of Fmoc-Gly (1.78 g, 8 equiv; Novabiochem, San Diego, CA) with diisopropylcarbodiimide (DIPCDI; 0.469 mL, 4 equiv; Aldrich, Milwaukee, WI) in dimethylformamide (DMF; 10 mL, anhydrous; Aldrich) and dichloromethane (DCM; 4 mL, anhydrous; Aldrich) for 30 min at room temperature with stirring under argon. The PEG (15 g, 1 equiv) was dissolved in DCM (30 mL). (Dimethylamino)pyridine (91.6 mg, 1 equiv; Novabiochem) in DCM (5 mL) was added to the dissolved PEG, and the resulting solution was added to the Fmoc-Gly anhydride. The vessel that contained the PEG was washed with 5 mL of DCM, which was also added to the reaction mixture. The reaction proceeded for 6 h at room temperature with stirring under argon. The reaction mixture was filtered through paper under vacuum and then precipitated in cold, rapidly stirred ether and collected by vacuum filtration. This resulting product constituted the zeroth-generation dendron copolymer. The reaction sequence detailed below was repeated five times to yield Dendron-5, a fifth-generation dendron copolymer.

Fmoc-Lys(Fmoc)-OH was added to the PEG as follows. Fmoc groups were removed from the PEG by dissolving the Fmoc-protected, lysine-grafted PEG in 20% piperidine in DMF (4 mL/g PEG 20K; Perseptive Biosystems, Framingham, MA), heating with swirling at 45 °C until it dissolved, and then allowing the mixture to stand at room temperature for 30 min. These steps were followed by precipitation in cold, stirred ether, vacuum filtration, and drying under vacuum, with 500 mg of each PEG-amine product retained. The Fmoc-amino acid (Fmoc-L-Lys(Fmoc)-OH; 3 equiv; Bachem, King of Prussia, PA) and HOBt (3 equiv; Novabiochem) were dissolved in DMF (3 mL/g of amino acid) and DCM (2 mL/g of amino acid). DIPCDI

(3 equiv) was added, and after 15 min, the PEG (2 mL DCM/g of PEG) was added (the vessel that contained the PEG solution was washed two times with 5 mL of DCM). The reaction proceeded with stirring at room temperature for at least 6 h under argon. The reaction mixture was then precipitated in stirred, cold ether, vacuum filtered, and dried under vacuum.

The dendron product was analyzed by gel permeation chromatography (GPC) at 1% in DMF (Polymer Laboratories PL-EMD 950 evaporative mass detector; Polymer Laboratories 5 μ m Mixed D 300 \times 7.5 and 5 μ m 500 Å 300 \times 7.5 in series columns; Polymer Laboratories, Amherst, MA). The chromatograms from the mass detector, which allowed a measurement of the mass of polymer, were compared with the UV adsorption at 300 nm (Fmoc absorption $\epsilon_{300} = 6558 \text{ L cm}^{-1} \text{ mol}^{-1}$) in order to calculate the percentage of coupling.

Plurionics F-108 NF and F-68 NF were obtained from BASF (Mount Olive, NJ).

2.2. Substrates. All of the waveguides used in this study were purchased from Microvacuum, Ltd. (Budapest, Hungary) and consisted of a 1-mm-thick AF45 glass substrate and a 200-nm-thick $\text{Si}_{0.4}\text{Ti}_{0.6}\text{O}_2$ waveguiding layer at the surface. For experiments involving titanium oxide and niobium oxide surfaces, an additional 14-nm-thick oxide layer was sputter coated in a Leybold dc-magnetron Z600 sputtering unit onto the waveguiding layer. All of these surfaces were characterized by XPS, AFM, and ToF-SIMS as previously reported.^{36,37,45}

Before each experiment, the waveguides were cleaned according to the following procedure: sonication in 0.1 M HCl for 10 min, extensive rinsing with ultra-high-purity water, and drying under nitrogen, followed by 2 min of oxygen-plasma cleaning in a Harrick Plasma Cleaner/Sterilizer PDC-32G instrument (Ossining, NY).

2.3. Experimental Techniques. **2.3.1. Optical Waveguide Lightmode Spectroscopy (OWLS).** The OWLS technique involves the incoupling of the evanescent field of a He–Ne laser into a planar waveguide that allows for the direct online monitoring of macromolecule adsorption. The method is highly sensitive (specifically, to $\sim 1 \text{ ng/cm}^2$) up to a distance of 100 nm above the surface of the waveguide. Furthermore, a measurement time resolution of 3 s allows for the in situ, real-time study of adsorption kinetics.

Areal adsorbed mass density data were calculated from the thickness and refractive index values derived from the mode equations³⁵ according to Feijter's formula. A refractive index increment (dn/dc) value of $0.182 \text{ cm}^3/\text{g}$ was used for the protein-adsorption calculations,^{35,46} and a value of $0.202 \text{ cm}^3/\text{g}$, as determined in a Raleigh interferometer, was used for the PLL-g-PEG adsorption calculations. All OWLS experiments were conducted in a BIOS-I OWLS instrument (ASI AG, Zurich, Switzerland) using a Kalrez (Dupont, Wilmington, DE) flow-through cell as described previously.^{36,45} The flow-through cell was used for studying both PLL-g-PEG adsorption and protein adsorption. The flow rate and wall shear rate were 1 mL/h and 0.83 s^{-1} , respectively.

2.3.2. X-ray Photoelectron Spectroscopy. X-ray photoelectron spectroscopy (XPS) analyses were performed using a PHI 5700 photoelectron spectrometer equipped with a concentric hemispherical analyzer in the standard configuration (Physical Electronics, Eden Prairie, MN). Spectra were acquired at a chamber pressure of 10^{-9} mbar using a non-monochromatized Al K α source operating at 200 W and positioned $\sim 13 \text{ mm}$ away from the sample. The analyzer was used in the fixed-analyzer transmission mode. Pass energies used for survey scans and

detailed scans were 187.85 and 23.5 eV, respectively. Under these conditions, the energy resolution [fwhm measured on silver Ag(3d5/2)] is 2.7 and 1.1 eV, respectively. Acquisition times were approximately 5 min for survey scans and 9 min for high-energy resolution elemental scans.

Angle-resolved XPS (AR-XPS) measurements were conducted at two different takeoff angles, namely 15° and 75° with respect to the surface plane, to obtain depth-dependent information on the molecular layers adsorbed onto the oxide substrate. (The typical sampling depths for 15° and 75° are 2–3 and 5–8 nm, respectively.) Spectra were referenced to the Ti(2p3/2) signal at 458.5 eV. Data were analyzed using a least-squares fitting routine following Shirley iterative background subtraction. Measured intensities (peak areas) were transformed into atomic concentrations by taking into account the respective atomic photoionization cross sections corresponding to PHI sensitivity factors⁴⁷ and by correcting for transmission functions and asymmetry factors. Spectra were fitted with the PC-Access V6.0F PHI software using the sum of a 90% Gaussian and 10% Lorentzian function.

2.4. Protocol for the Adsorption Experiments. **2.4.1. Protocol for XPS Sample Preparation.** Prior to XPS analysis, the samples were ultrasonically cleaned in 0.1 M HCl for 10 min, extensively rinsed with ultra-high-purity water, and dried in a nitrogen stream, followed by 2 min of oxygen-plasma cleaning, as described earlier. PLL-g-PEG-modified surfaces were prepared by dip coating for 10 min in a 1 mg/mL solution of PLL-g-PEG in 10-mM HEPES [4-(2-hydroxyethyl)piperazine-1-ethanesulfonic acid, adjusted to pH 7.4 with 1 M NaOH solution]. This buffer solution will be referred to as HEPES Z1 hereafter. Subsequently, the modified waveguides were rinsed immediately with ultrapure water and dried under nitrogen. Some samples were analyzed and used without the proper cleaning step described in the sample preparation procedure to test the effect of surface contamination on the adsorption and subsequent performance of PLL-g-PEG.

2.4.2. Protocol for OWLS Experiment and Sample Preparation. Samples with adsorbed PLL-g-PEG layers were prepared as described in section 2.4.1 and dried in flowing nitrogen. Their protein- and serum-adsorption performance was subsequently measured by OWLS as described later in section 2.4.3.

Samples modified with PLL-g-PEG in situ were initially placed in HEPES Z1 immediately following the cleaning procedure and allowed to soak overnight. Prior to assembly of the flow-through cuvette in the OWLS instrument, the samples were rinsed with ultrapure water and dried under nitrogen. These presoaked samples equilibrated and reached a flat baseline in HEPES Z1 in less than 1 h. Then, the samples were exposed, in situ, to the PLL-g-PEG solution (1 mg/mL in HEPES Z1). The adsorption was subsequently monitored for 30 min. The polymer solution was then replaced with HEPES Z1, and the protein- and serum-adsorption performance was measured as described later in section 2.4.3.

$\text{Si}_{0.4}\text{Ti}_{0.6}\text{O}_2$ waveguides were used for the pH-dependence measurements and were prepared as described in the immediately preceding procedure. However, in this case, the solution consisted of 10 mM HEPES, titrated to the predetermined pH by the addition of either 1 M NaOH or 1 M HCl. The polymer concentration was 0.1 mg/mL in the same pH-adjusted HEPES solution. After 1 h of polymer adsorption and 30 min of washing with the pH-adjusted solution, the solution was changed to the pH 7.4 buffer (HEPES Z1), and the protein-adsorption performance was measured, as described in section

TABLE 2: XPS Binding Energies/Peak Areas and Surface Concentrations for Cleaned, Contaminated, and PLL(375)-g[5.6]-PEG(5)-Modified TiO₂ Surfaces

surface	angle of detection [°](deg)	atomic concentration (atom %)					binding energy (eV) (relative peak area (%))					
		C	O	Ti	N	Si	C1s _A C—C, C—H	C1s _B C—O	C1s _C NHC(=O) O—C=O	O1s _A TiO ₂	O1s _B COO*, OH	O1s _C C—O, H ₂ O
clean TiO ₂	15	34.5	49.8	15.7	—	—	284.9 (76.5)	286.6 (13.9)	288.7 (9.6)	530.0 (67.1)	531.5 (23.9)	532.7 (9.0)
	75	12.7	63.7	23.6	—	—	284.9 (70.2)	286.6 (16.7)	288.7 (13.1)	530.0 (77.3)	531.5 (17.1)	532.7 (5.6)
PLL(375)- g(5.6)-PEG(5)- covered TiO ₂	15	52.5	41.8	5.0	0.7	—	285.1 (14.6)	286.7 (75.6)	288.5 (9.8)	530.0 (24.6)	531.4 (16.7)	532.9 (58.7)
	75	26.7	55.7	16.6	1.0	—	285.1 (16.1)	286.7 (72.5)	288.5 (11.4)	530.0 (62.0)	531.4 (16.2)	532.9 (21.8)
contaminated TiO ₂	15	47.0	38.5	10.1	0.5	3.9	284.9 (89.5)	286.6 (7.4)	289.1 (3.1)	530.3 (66.7)	531.9 (26.0)	533.0 (7.3)
	75	15.6	59.0	21.5	0.4	3.5	284.9 (86.8)	286.6 (9.7)	289.1 (3.5)	530.3 (85.9)	531.9 (14.1)	—
PLL(375)- g(5.6)-PEG(5)- covered contaminated TiO ₂	15	69.8	25.1	2.7	1.6	0.8	285.4 (59.9)	286.9 (33.9)	288.6 (6.2)	530.4 (26.7)	531.6 (5.5)	533.2 (67.8)
	75	35.7	46.0	15.1	1.7	1.5	285.4 (58.0)	286.9 (34.4)	288.6 (7.6)	530.4 (70.6)	531.6 (10.1)	533.2 (19.3)
theoretical PLL(375)- g(5.6)-PEG(5)		66.7	30.0	—	3.3	—	285.0 (13.3)	286.5 (83.8)	288.1 (2.9)	—	531.6 (6.5)	532.8 (93.5)

2.4.3. The same procedure was used for the ionic-strength-dependence experiments, except that NaCl was used to generate the solution of predetermined ionic strength.

2.4.3. Protocol for Protein-Adsorption Experiments. The waveguides were exposed to a solution of human serum (Control Serum N, Art.# 07 3711 9, US# 42384, Roche, Basel, Switzerland) for 1 h at a temperature of 25 °C and subsequently washed for 30 min in HEPES Z1.

Human serum albumin (HSA) and human fibrinogen were obtained from Sigma Chemical Co., and their related antibodies were obtained from Dako A/S (Glostrup, Denmark). In the case of the single protein-adsorption experiments, the waveguide was exposed to a 1 mg/mL solution of the appropriate protein in HEPES Z1 for 1 h at a temperature of 25 °C and subsequently washed for 30 min in HEPES Z1.

In some cases, after the serum exposure, the waveguide was tested against solutions of 0.1 mg/mL rabbit anti-HSA and 0.28 mg/mL rabbit anti-human fibronectin for 30 min at a temperature of 25 °C and subsequently washed for 30 min in HEPES Z1. Adsorption of human fibrinogen was tested separately by exposure to a 1 mg/mL solution of fibrinogen for 1 h at 25 °C followed by exposure to a 0.1 mg/mL solution of rabbit anti-human fibrinogen for 30 min.

3. Results

3.1. Surface Characterization of Unmodified and Modified Waveguides. **3.1.1. X-ray Photoelectron Spectroscopy.** X-ray photoelectron spectroscopy was performed at two different detection angles (75° and 15° relative to the surface plane) on a variety of untreated and treated titanium oxide (TiO₂) surfaces, specifically, contaminated (not plasma-cleaned), plasma-cleaned, contaminated and treated with PLL(375)-g[5.6]-PEG(5), and plasma-cleaned and treated with PLL(375)-g[5.6]-PEG(5). The quantitative results of the XPS study are summarized in Tables 2 and 3. Figure 2 shows the most relevant detail spectra, that is, the C(1s) and O(1s) spectra of the clean TiO₂ surface and of the clean TiO₂ surface with adsorbed PLL-g-PEG at the two different detection angles.

TABLE 3: Atomic Ratios Calculated from XPS Data for PLL(375)-g[5.6]-PEG(5)-Modified TiO₂ Surfaces^a

surface	angle of detection [°](deg)	atomic ratio				
		C _B /C _A ^c	O _C /O _A ^c	O _A /Ti ^c	C _B /O _C ^c	O _C /N ^c
PLL(375)- g(5.6)-PEG(5)- covered TiO ₂	15	5.2	2.4	2.12	1.98	34.4
	75	4.5	0.35	2.06	1.95	10.5
PLL(375)- g(5.6)-PEG(5)- covered contaminated TiO ₂	15	0.57	2.5	2.4	1.53	14.0
	75	0.59	0.27	2.2	2.09	4.5
theoretical ^b PLL(375)- g(5.6)-PEG(5) on TiO ₂		6.3	—	2.0	2.0	8.3

^a A homogeneous elemental distribution is assumed. ^b Theoretical values expected for the stoichiometry of the polymer. ^c Contributions A, B, and C are defined in Table 2 above.

A rough quantification based on the overall detected intensities of the elements (when not distinguishing between different chemical states) shows the effect of the cleaning procedure on the remaining surface contamination (see Tables 2 and 3). At a 15° detection angle, the carbon concentration at the oxide surface (mainly adventitious hydrocarbon) clearly decreased from 47.0 to 34.5 atom % after plasma cleaning. The latter value is considered to be typical for well-cleaned surfaces.³⁷ After adsorption of PLL(375)-g[5.6]-PEG(5) on both types of surfaces, the carbon concentration significantly increased, as expected. The overall oxygen concentration showed less variation between uncoated and coated surfaces, as both the organic PLL(375)-g[5.6]-PEG(5) overlayer and the titanium oxide substrate contain high levels of oxygen. In comparing the data from spectra taken at 15° and 75° detection angles, one finds appreciably higher carbon concentrations in the case of the grazing exit angle (15°). This is a clear confirmation that both the adventitious contamination and the PLL(375)-g[5.6]-PEG(5) adlayer were located on top of the titanium oxide surface, because the information depth of the XPS technique is much lower for the 15° arrangement than for the 75° arrangement.

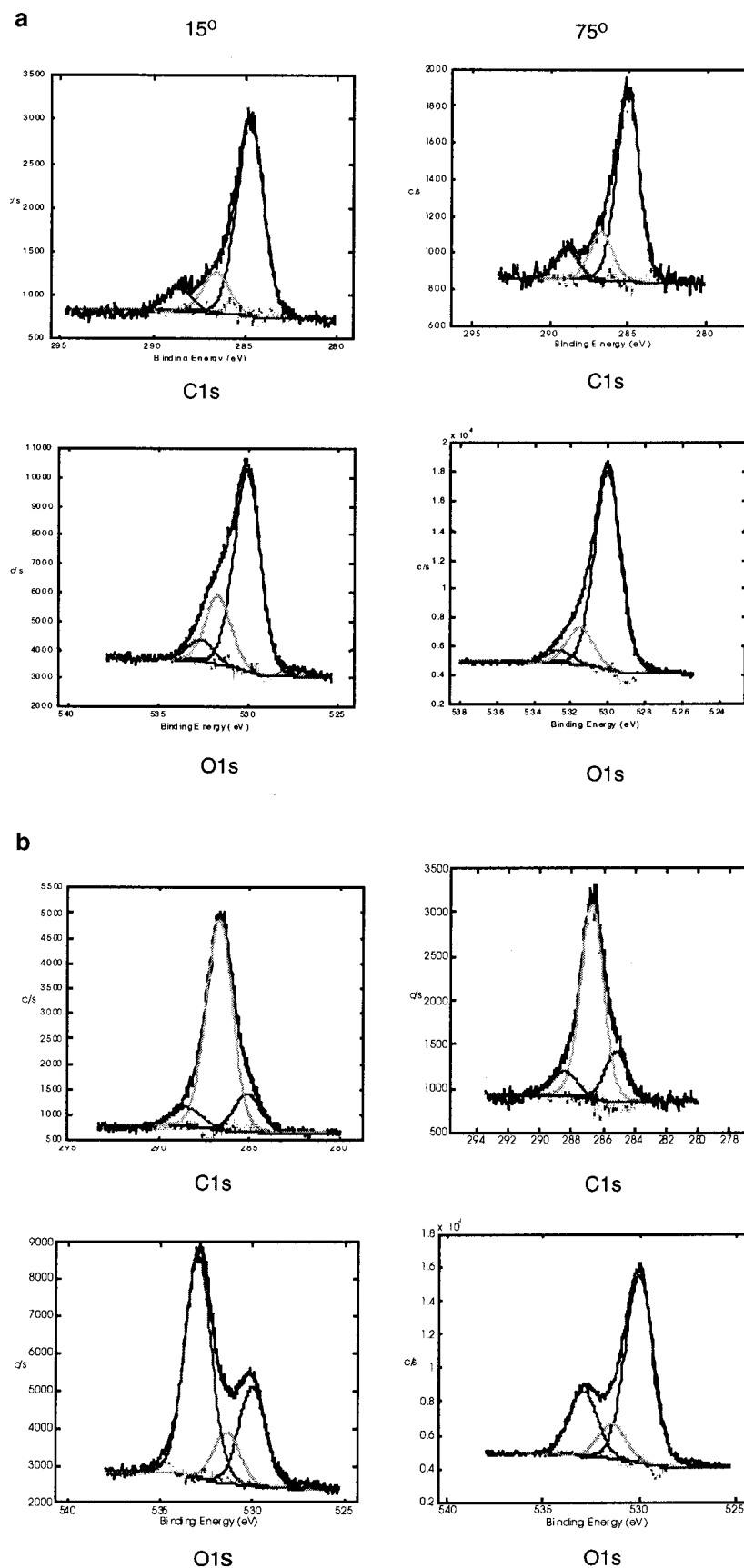


Figure 2. Detail XPS spectra in the C(1s) and O(1s) region at the two different detection angles (relative to the surface plane) of 15° (more surface-sensitive) and 75° (less surface-sensitive): (a) plasma-cleaned TiO₂ surface and (b) plasma-cleaned TiO₂ surface coated with PLL(375)-g[5.6]-PEG(5).

The data based on the high-resolution spectra, presented in Tables 2 and 3 and Figure 2, provide more detailed insight into

the surface architecture of the PLL(375)-g[5.6]-PEG(5)-modified titanium oxide surfaces. Both carbon and oxygen were detected

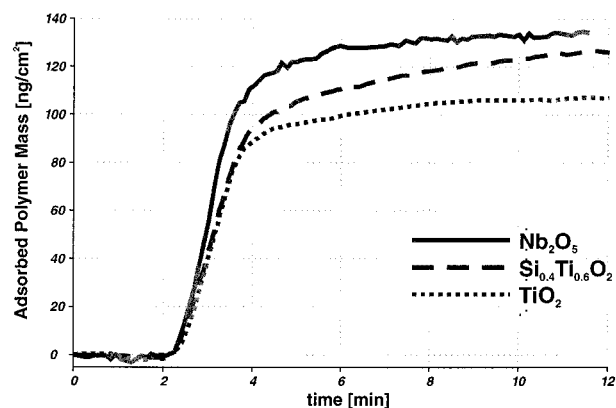


Figure 3. Examples of PLL(375)-g[5.6]-PEG(5) adsorption curves on three metal oxide surfaces, as measured by the OWLS technique [10 mM HEPES Z1 (pH 7.4), 1 mg/mL polymer, 1 mL/h, $T = 26^\circ\text{C}$].

in different chemical states, and the deconvoluted peaks were assigned to particular molecular functionalities on the basis of existing experience and published reference data.⁴⁷ Further discussion of the XPS results is presented in section 4.

3.2. PLL(375)-g[5.6]-PEG(5) Adsorption and Protein-Resistance Study. **3.2.1. PLL(375)-g[5.6]-PEG(5) Adsorption Characteristics.** All of the following measurements were carried out in a flow-through cell, and both the PLL-g-PEG pretreatment and the protein-adsorption tests were carried out in situ and consecutively without an intermittent drying stage unless otherwise noted.

The results of the OWLS experiments (see Figure 3) indicate that the PLL-g-PEG polymer spontaneously adsorbed from a pH 7.4 buffered aqueous solution onto metal oxide surfaces. The example shown in Figure 3 involved the adsorption of PLL-g-PEG onto three different metal oxide surfaces, specifically, titanium, niobium, and silicon/titanium. This adsorption process occurred rapidly and resulted in the formation of a layer of adsorbed polymer on the surface. Typically, for $\text{Si}_{0.4}\text{Ti}_{0.6}\text{O}_2$ surfaces, a layer with an adsorbed areal density of approximately 125 ng/cm^2 formed, and 95% of the final observed mass was reached within the first 5 min. Similar behavior was observed for the two other metal oxide surfaces investigated (that is, niobium pentoxide and titanium dioxide). Although the adsorption kinetics were quite similar, the resulting amount of PLL-g-PEG adsorbed to the surface was different and depended on the characteristic isoelectric point of the metal oxide, as shown in Figure 4 and Table 4.^{37,38,46,48,49}

3.2.2. Protein-Adsorption Characteristics of PLL(375)-g[5.6]-PEG(5)-Modified Surfaces. Subsequent protein-adsorption experiments revealed that PLL-g-PEG modification of the metal oxide surfaces resulted in sharply reduced protein adsorption. Typically, the exposure of a metal oxide surface to serum

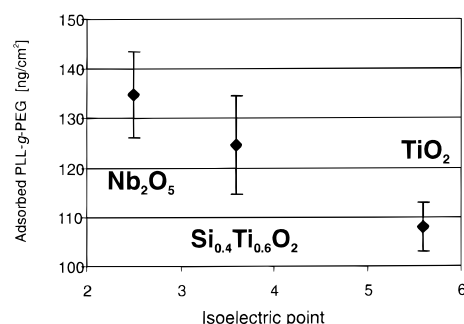


Figure 4. Dependence of the adsorbed amount of PLL(375)-g[5.6]-PEG(5) on the isoelectric point of the metal oxide surfaces, as measured by the OWLS technique [10 mM HEPES Z1 (pH 7.4), 1 mg/mL polymer, 1 mL/h, $T = 26^\circ\text{C}$].

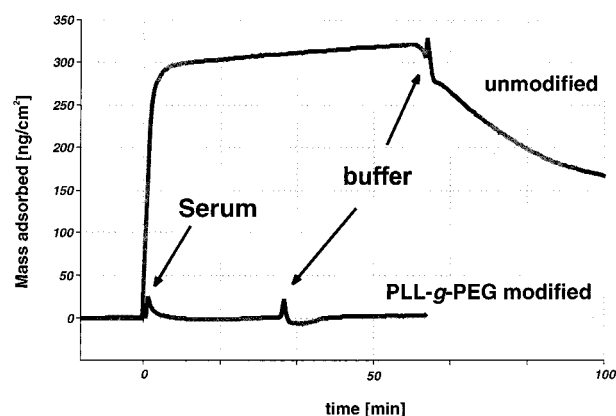


Figure 5. Serum-adsorption spectrum of an unmodified and a PLL(375)-g[5.6]-PEG(5)-modified $\text{Si}_{0.4}\text{Ti}_{0.6}\text{O}_2$ surface, as measured by the OWLS technique [PBS (pH 7.4), 1 mg/mL polymer, $T = 26^\circ\text{C}$]. The baseline was achieved under PBS, and the spikes are due to temporary flow rate-related pressure changes.

produces a layer of adsorbed protein with an areal density of between 150 and 250 ng/cm^2 after the washing step.⁵⁰ However, waveguides that are precoated with a layer of PLL-g-PEG show a drastic reduction in subsequent serum protein adsorption. An example of this is shown in Figure 5. This experiment involved modified and unmodified silicon/titanium dioxide waveguides that were prepared according to the procedure described in section 1.4.1. Generally, PLL(375)-g[5.6]-PEG(5) pretreatment, regardless of the preparation procedure, caused an order-of-magnitude decrease in the areal density of adsorbed protein following serum exposure on titanium dioxide, silicon/titanium dioxide, and niobium oxide surfaces (see Figure 6). Moreover, the adsorption of human serum albumin (1 mg/mL, 10 mM HEPES-buffered solution, pH 7.4) was decreased by two orders of magnitude following the PLL-g-PEG pretreatment (see Figure

TABLE 4: Summary of the Isoelectric Points and the Charge Densities^{46,49} of Investigated Surfaces and the Observed Adsorbed Areal Density of PLL(375)-g[5.6]-PEG(5), Serum, and Human Serum Albumin (HSA) on Unmodified Surfaces and of Serum and HSA on PLL(375)-g[5.6]-PEG(5)-Modified Surfaces^a

substrate	isoelectric point	surface charge at pH 7.4 (uC/cm ²)	adsorbed mass of PLL(375)-g(5.6)-PLL(5) (ng/cm ²)	adsorbed mass of serum on an untreated surface (ng/cm ²)	adsorbed mass of serum on a PLL(375)-g(5.6)-PLL(5)-treated surface (ng/cm ²)	adsorbed mass of HSA on an untreated surface (ng/cm ²)	adsorbed mass of HSA on a PLL(375)-g(5.6)-PLL(5)-treated surface (ng/cm ²)
TiO ₂	5.6	5	108 ± 9	320 ± 31	20 ± 40	200 ± 20	<1.0
$\text{Si}_{0.4}\text{Ti}_{0.6}\text{O}_2$	3.6	25	125 ± 13	596 ± 89	25 ± 5	176 ± 10	<1.0
Nb ₂ O ₅	2.5	50	135 ± 13	445 ± 8	19 ± 22	96 ± 70	24 ± 16

^a Polymer adsorption carried out under 10 mM HEPES Z1, 1 mg/mL polymer, 1 mL/h, $T = 26^\circ\text{C}$; serum adsorption, 1 mL/h, $T = 26^\circ\text{C}$; HSA adsorption, 10 mM HEPES Z1, 1 mg/mL HSA, 1 mL/h, $T = 26^\circ\text{C}$.

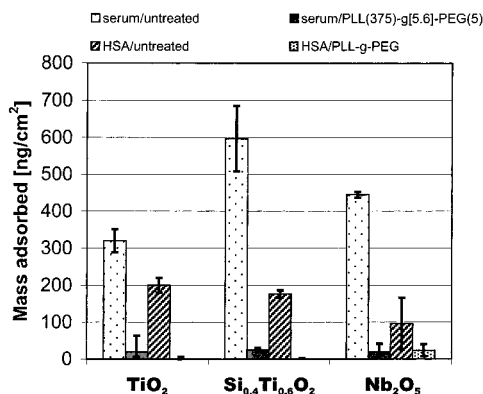


Figure 6. Adsorbed areal mass of serum and HSA on PLL(375)-g[5.6]-PEG(5)-modified and unmodified Si_{0.4}Ti_{0.6}O₂, TiO₂, and Nb₂O₅ surfaces, as measured by the OWLS technique [10 mM HEPES Z1 (pH 7.4), 1 mg/mL polymer, 1 mL/h, $T = 26\text{ }^{\circ}\text{C}$].

6). The quantitative protein-adsorption data for all surfaces studied are listed in Table 4.

The residual material remaining on the surface after serum exposure was tested against antibodies of several common serum proteins, such as anti-albumin, anti-fibronectin, and anti- γ -globulin. Each of these antibodies exhibited an adsorbed areal density lower than the detection limit of the OWLS technique (that is, $<2\text{ ng/cm}^2$), which suggests that none of the proteins are present in their active conformations on the modified surfaces. It is likely that serum components other than proteins are picked up by the modified surfaces. Because serum is fibrinogen-depleted, fibrinogen was also tested separately from a 5 mg/mL solution in HEPES Z1, followed by an anti-fibrinogen assay. For a PLL(375)-g[5.6]-PEG(5)-modified silicon/titanium dioxide surface, 85 and 150 ng/cm² of adsorbed areal density was observed for fibrinogen and anti-fibrinogen, respectively. The antibody results are not shown.

3.2.3. Model of the PLL(375)-g[5.6]-PEG(5)/Surface Oxide Interaction. The adsorption of PLL(375)-g[5.6]-PEG(5) was found to be dependent on electrostatic interactions. The observation that the limiting mass of PLL-g-PEG adsorption increases for surfaces of decreasing isoelectric points provides evidence that the mechanism of surface adsorption is of an electrostatic nature (see Figures 3 and 4). By varying the pH of the solution in contact with the surface of the waveguide, one can control the sign and density of the surface charge. For example, at pH values lower than the isoelectric point of the metal oxide, the surface bears a positive charge, and at pH values higher than the isoelectric point, the surface bears a negative charge. Similarly, because the PLL backbone of this graft copolymer contains primary amines with a pK_a of about 10, pH values below 10 lead to a net positive charge on the polymer backbone, whereas pH values well above 10 render the polymer backbone essentially uncharged.

Maximal polymer adsorption occurs within a pH range between the isoelectric point of the surface and the pK_a of the polymer. Experiments performed at different pH values, as described in section 2.4.2, showed that negligible PLL-g-PEG adsorption is observed at pH values higher than the pK_a of the polymer (pH ~ 10) or lower than the isoelectric point of the metal oxide surface. The experimental data shown in Figure 7 demonstrate that, for a silicon/titanium dioxide surface, PLL-g-PEG adsorption takes place only in the pH range between 3 and 11. Outside of this range, negligible adsorption is observed.

The surfaces were found to exhibit suppression of protein adsorption only when an appreciable layer of PLL(375)-g[5.6]-PEG(5) was present at the surface. This behavior was observed

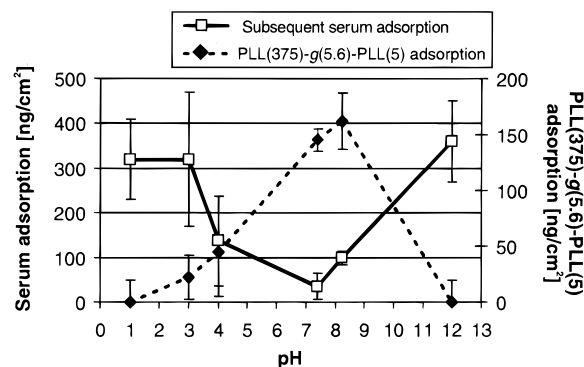


Figure 7. pH dependence of PLL(375)-g[5.6]-PEG(5) and subsequent serum adsorption on Si_{0.4}Ti_{0.6}O₂ surfaces, as measured by the OWLS technique [polymer adsorption carried out under titrated 10 mM HEPES Z1, 1 mg/mL polymer, 1 mL/h, $T = 26\text{ }^{\circ}\text{C}$; serum adsorption, 1 mL/h, $T = 26\text{ }^{\circ}\text{C}$].

for experiments involving the adsorption of human serum onto a modified silicon/titanium dioxide surface, as shown in Figure 7. Clearly, suppression of protein adsorption depended on the presence of a preadsorbed layer of PLL(375)-g[5.6]-PEG(5). The same general behavior was observed for human serum albumin adsorption onto modified titanium dioxide surfaces.

Experiments involving the adsorption of PLL(375)-g[5.6]-PEG(5) onto the surface of titanium oxide waveguides from solutions of varying ionic strength showed the adsorption to be ionic-strength dependent. An increase in the ionic strength of the PLL(375)-g[5.6]-PEG(5) solution brought about a decrease in the surface areal density of resulting adsorbed polymer. At ionic strengths above 2 M, negligible adsorption was observed. Importantly, an adsorbed areal density of 130 ng/cm² was observed at an ionic strength of 150 mM, the physiological ionic strength. Furthermore, this adsorbed layer of PLL(375)-g[5.6]-PEG(5) demonstrated an order-of-magnitude decrease in the subsequent serum protein adsorption (specifically, $\sim 25\text{ ng/cm}^2$), a performance equivalent to that of the polymer layer adsorbed from 10-mM ionic-strength solution.

Exposure of a preadsorbed layer of PLL(375)-g[5.6]-PEG(5) to a solution with a pH value outside of the pH range where adsorption is observed or to a solution with a high ionic strength causes a gradual desorption of the polymer. Therefore, the adsorption of PLL(375)-g[5.6]-PEG(5) and the stability of this adsorbed polymer layer require that the contacting solution be limited to the pH range between the isoelectric point of the surface and the pK_a of the polymer, and to low ionic strengths.

3.2.4. Performance and Long-Term Stability of the Adsorbed PLL(375)-g[5.6]-PEG(5) Layer. Once established on the surface, the adsorbed layer of PLL(375)-g[5.6]-PEG(5) was found to be stable (that is, $<5\%$ loss in mass of the adsorbed layer after 1 week) and resistant to protein adsorption over 24 h at 37 $^{\circ}\text{C}$ under a flowing HEPES Z1 solution, as shown in Figure 8. This experiment involved the in situ deposition, within the first hour, of a PLL(375)-g[5.6]-PEG(5) layer on the surface of a silicon/titanium dioxide waveguide. Two subsequent exposures to serum produced less than 20 ng/cm² of surface-adsorbed protein. Eighteen hours later, two additional serum exposures similarly produced less than 20 ng/cm². Similar performance was observed when PBS was used as the buffer instead of HEPES Z1.

PLL(375)-g[5.6]-PEG(5)-modified waveguides that were stored dry were found to retain their protein-resistant properties after more than 3 months, and those stored in HEPES-buffered solution were found to retain their protein-resistant properties after more than 1 month.

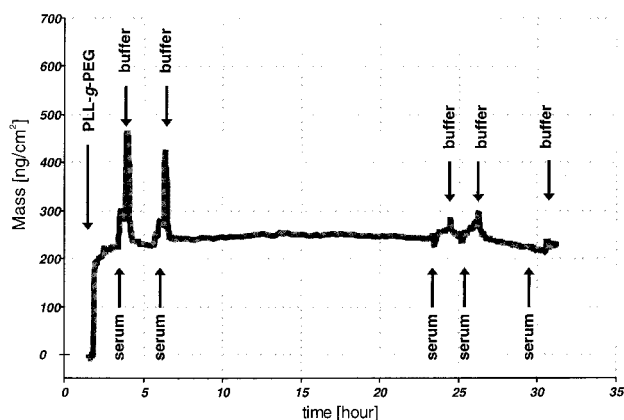


Figure 8. Long-term stability of the protein-adsorption suppression of a PLL(375)-g[5.6]-PEG(5)-modified $\text{Si}_{0.4}\text{Ti}_{0.6}\text{O}_2$ surface, as measured by the OWLS technique [polymer adsorption carried out under 10 mM HEPES Z1, 1 mg/mL polymer, 1 mL/h, $T = 26^\circ\text{C}$; serum adsorption, 1 mL/h, $T = 26^\circ\text{C}$].

Pluronics, diblock copolymers consisting of poly(propylene oxide) flanked by two poly(ethylene oxide) chains, are commonly used to immobilize PEG on hydrophobic surfaces. However, Pluronics F-108 and F-68 were found not to adsorb onto any of the metal oxide surfaces investigated here and, as a result, did not show any protein-adsorption-suppressing properties.

PLL(375)-g[5.6]-PEG(5) was also found to adsorb onto a preadsorbed layer of serum proteins. After a typical adsorption of serum protein (that is, about 260 ng/cm^2), subsequent exposure to a 1 mg/mL solution of PLL(375)-g[5.6]-PEG(5) effected an overlayer of polymer with a surface areal density of approximately 90 ng/cm^2 .

3.2.5. Effect of Precontamination on PLL(375)-g[5.6]-PEG(5) Adsorption. Metal oxide surfaces that exhibited large amounts of hydrocarbon surface contamination nevertheless adsorbed a layer of PLL(375)-g[5.6]-PEG(5) that suppressed subsequent serum adsorption. Titanium dioxide waveguides that were not cleaned according to the procedure described in section 1.4.1 exhibited substantial hydrocarbon surface contamination (see Tables 2 and 3 and Figure 2). However, these XPS data also indicate that an additional layer of PLL(375)-g[5.6]-PEG(5) does, indeed, adsorb onto this contaminated surface. Furthermore, OWLS experiments showed that the typical adsorbed areal density of 120 ng/cm^2 forms on contaminated titanium dioxide waveguides and that this adsorbed layer of polymer suppresses subsequent serum protein adsorption by about 95%. That is, the adsorption and performance characteristics of PLL(375)-g[5.6]-PEG(5) are identical in the case of both contaminated and cleaned titanium dioxide surfaces.

3.3. Effect of Polymer Architecture. Alternative architectures of the polymer were explored for the suppression of protein-adsorption performance. These architectures included comblike graft copolymers with differing PEG side-chain length, PLL backbone length, and PEG grafting ratio (see Table 1). The inverted tree-like dendrimeric PLL having a single PEG side chain attached at the base was also investigated.

3.3.1. Effect of the Backbone (PLL) Structure on Subsequent Protein Adsorption. The graft copolymer architecture was found to influence the subsequent serum-adsorption suppression. All of the polymers investigated demonstrate adsorption on silicon/titanium dioxide surfaces in the areal density range of about 150 ng/cm^2 , as shown in Figure 9. Of the two comb copolymers with PEG side chains of mol wt 5000, PLL(375)-g[5.6]-PEG(5) demonstrates only a slightly more pronounced suppression

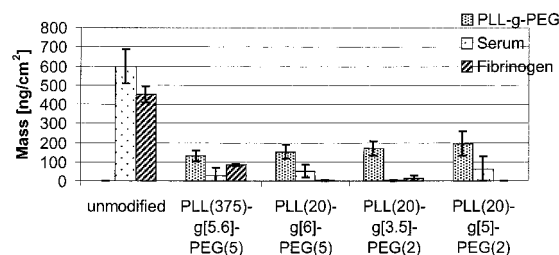


Figure 9. Effect of polymer architecture on the adsorbed areal density of the copolymer and subsequent serum and fibrinogen on $\text{Si}_{0.4}\text{Ti}_{0.6}\text{O}_2$ surfaces as measured by the OWLS technique [polymer adsorption carried out under 10 mM HEPES Z1, 1 mg/mL polymer, 1 mL/h, $T = 26^\circ\text{C}$; serum adsorption, 1 mL/h, $T = 26^\circ\text{C}$].

TABLE 5: Observed Adsorbed Areal Density of Polymer, Serum, and Fibrinogen on $\text{Si}_{0.4}\text{Ti}_{0.6}\text{O}_2$ Surfaces Modified with Various PLL-g-PEG Copolymers^a

	adsorbed mass of PLL-g-PEG polymer (ng/cm^2)	adsorbed mass of serum (ng/cm^2)	adsorbed mass of fibrinogen (ng/cm^2)
unmodified $\text{Si}_{0.4}\text{Ti}_{0.6}\text{O}_2$	—	596 ± 89	451 ± 42
PLL(375)-g[5.6]-PEG(5)	133 ± 28	30 ± 42	85 ± 5
PLL(20)-g[6]-PEG(5)	152 ± 35	50 ± 33	3 ± 2.5
PLL(20)-g[3.5]-PEG(2)	169 ± 36	3 ± 4	15 ± 14
PLL(20)-g[5]-PEG(2)	194 ± 63	63 ± 63	1 ± 1

^a Polymer adsorption carried out under 10 mM HEPES Z1, 1 mg/mL polymer, 1 mL/h, $T = 26^\circ\text{C}$; serum adsorption, 1 mL/h, $T = 26^\circ\text{C}$; fibrinogen adsorption, 10 mM HEPES Z1, 1 mg/mL fibrinogen, 1 mL/h, $T = 26^\circ\text{C}$.

of serum adsorption, decreasing the observed adsorption by about 95% to 30 ng/cm^2 . The graft copolymer with the lower molecular weight, PLL(20)-g[6.0]-PEG(5), decreases the observed protein adsorption from serum exposure by about 90% to 50 ng/cm^2 . Dendron-5, consisting of a 20 000 mol wt PEG with a terminus consisting of a fifth-generation lysine dendrimer, was also found to adsorb onto silicon/titanium dioxide surfaces in the areal density range of 120–150 ng/cm^2 . Furthermore, this adsorbed polymer layer was found to decrease the subsequent protein adsorption due to serum exposure by about 85% to 80 ng/cm^2 .

3.3.2. Effect of the Copolymer Grafting Ratio on Subsequent Protein Adsorption. The grafting ratios that were investigated were found to have only a slight influence on the subsequent serum-adsorption performance. To explore the effect of the grafting ratio on the polymer adsorption and subsequent protein-resistance behavior, PLL(20)-g[3.5]-PEG(2) and PLL(20)-g[5]-PEG(2) were synthesized. These two polymers differ only in their respective grafting ratios of 3.5/1 and 5.0/1 (where the ratio is for lysine monomer to PEG side chain). As shown in Figure 9, PLL(20)-g[3.5]-PEG(2) and PLL(20)-g[5]-PEG(2) exhibited adsorbed mass densities of 170 and 190 ng/cm^2 , respectively. PLL(20)-g[3.5]-PEG(2) appears to have a slightly greater suppression of protein adsorption [specifically, a 99% decrease to 3 ng/cm^2 vs a 90% decrease to 63 ng/cm^2 for PLL(20)-g[5]-PEG(2)], but the differences actually are not statistically significant. In many of the experiments involving both of these polymers, this amount of adsorbed mass was close to the detection limit of the OWLS technique (~ 2 ng/cm^2) (see Table 5).

3.3.3. Coadsorption Effects on Overall Graft Copolymer Adsorption. Coadsorption effects were explored by varying the sequence of polymer types exposed to the surface, as well as by mixing the polymer types, and then observing the dependence

of the behavior of the adsorbed polymer layer. No significant coadsorption effects were observed. For example, exposing a layer of preadsorbed high-molecular-weight graft copolymer to a solution of low-molecular-weight graft copolymer showed no increase in adsorbed polymer mass and no change in subsequent protein-adsorption behavior from that of the preadsorbed layer alone. Furthermore, exposing a layer of preadsorbed low-molecular-weight graft copolymer to a solution of high-molecular-weight graft copolymer showed no increase in adsorbed polymer mass and no change in subsequent protein-adsorption behavior from that of the preadsorbed layer alone. Exposing the surface to a solution containing a mixture of both polymers showed the same adsorbed areal density and protein-adsorption resistance as that of a layer of high-molecular-weight graft copolymer alone.

4. Discussion

In this study, the adsorption of polyelectrolytes, such as the class of PLL-*g*-PEG graft copolymers on metal oxide surfaces, was found to be consistent with the related observations from previous studies. In previous characterizations of the adsorption behavior of polyelectrolytes on such metal oxide surfaces, polycations in particular, such as PLL, were found to form stable adsorbed layers on negatively charged oxides such as silicon dioxide and titanium dioxide.^{21–23} However, the class of PLL-*g*-PEG-based copolymers thus far had been evaluated only in the contexts of drug delivery^{32,33} and the reduction of cell adhesion^{24–27,34} without a thorough characterization of the related modified surfaces and their reduction of protein adsorption.

4.1. Adsorption and Structure of the PLL-*g*-PEG Adlayer.

The adsorption behavior of the class of PLL-*g*-PEG graft copolymers investigated here was evaluated by means of XPS. In the case of the uncoated TiO₂ surfaces, the C(1s) spectrum is dominated by an adventitious hydrocarbon emission (binding energy of ~285.0 eV), whereas the O(1s) spectrum shows a contribution that is characteristic of the titanium oxide substrate (binding energy of ~530 eV). However, there are additional contributions at higher binding energies in both the C(1s) and the O(1s) spectra, which are believed to be derived from oxygen-containing organic contaminants, hydroxide groups, and water molecules that are present at the titanium surface. As expected, these additional surface species are more pronounced in the more surface-sensitive 15° spectra (see Figure 2), as is the case for all species that are presumably located at the outermost layer. The quantitative ratio of O(TiO₂)/Ti is slightly higher than expected but close to the stoichiometric value of 2.0 (Table 3).

In the case of PLL(375)-*g*[5.6]-PEG(5) coated on the clean TiO₂ surfaces, both the carbon and the oxygen signals appear quite different from the corresponding signals in the bare TiO₂ spectra. The C(1s) region is now dominated by a peak at ~286.7 eV, which is typical for the C—O—C entity that is present in PEG (see Figure 1). Similarly, the O(1s) spectra show substantial intensities at the binding energy of ~533 eV, which is assigned to the O atoms of the PEG chains. Both the O(TiO₂)/Ti and the C(PEG)/O(PEG) ratios are close to the expected ratio of 2.0, providing further evidence that the curve fitting and the assignment of spectral components to functionalities at the surface is, indeed, reasonable (Tables 2 and 3). The species assigned to —NHC(=O) in the C(1s) and O(1s) spectra have higher intensities than would be expected from the stoichiometry of the PLL-*g*-PEG (Tables 2 and 3) polymer. This discrepancy is primarily due to the fact that the bare TiO₂ surfaces also show emission peaks in the same specific energy ranges (288–289

and 531–532 eV) from O-containing natural organic contaminants and OH species at the surface of the titanium oxide. The ratio of O(C—O—C)/N determined at a detection angle of 75° (10.5) is only slightly higher than the theoretical value of 8.3 for the stoichiometric ratio of the PLL(375)-*g*[5.6]-PEG(5) molecule. A higher value would be expected if the nitrogen atoms were preferentially located at the surface of the TiO₂. Indeed, at the detection angle of 15°, this value is much higher (34), which would be expected for a polymer configuration with the amine groups of the PLL backbone located at or close to the interface and the PEG chains located preferentially above the PLL polymer.

The sample with PLL(375)-*g*[5.6]-PEG(5) adsorbed onto the contaminated TiO₂ surface shows a much higher proportion of hydrocarbon contamination than the sample with PLL-*g*-PEG adsorbed onto a clean oxide surface (see Tables 2 and 3, C(1s) contribution at a binding energy of 285 eV). The ratio of C(PEG)/C(C—C) in Table 3 can be taken as a rough measure of the ratio of the amount of PEG to the amount of adventitious hydrocarbon contamination; this ratio is approximately a factor 10 higher for the “clean case” than for the “contaminated case”. This finding implies that these contaminants are not displaced by PLL-*g*-PEG during the adsorption step. Nevertheless, the amount of PLL-*g*-PEG that is adsorbed onto the contaminated oxide surface is comparable to the amount adsorbed in the clean case. This can be roughly deduced in Table 3 from the ratio of O(PEG)/O(TiO₂), which is a sensitive function of PEG coverage. This ratio shows a similar value for the two cases (2.4–2.5 at the 15° detection angle and 0.3–0.4 at the 75° detection angle). The conclusion is that the surface contaminants are not displaced by the PLL-*g*-PEG molecules, but that the polymer molecules bridge across the contaminants at the surface and adsorb at a density comparable to that obtained in the clean case.

Complementary to the XPS studies, the OWLS technique was used in the present study to quantify the polymer and biomolecule adsorption. This technique has a detection limit of about 2 ng/cm². Furthermore, the OWLS technique is direct in that it does not require labeling or any other potentially property-altering modifications to the adsorbing species. The areal density of PLL(375)-*g*[5.6]-PEG(5) adsorbed onto the oxide surfaces was found to be only weakly dependent on the oxide surface charge density. As shown in Table 4, the surface charge density of titanium at a pH of 7.4 and an ionic strength of 10 mM is an order of magnitude lower than that of niobium, although the adsorbed areal density of the polymer on titanium was only 20% lower than that on niobium. As expected, spatial packing considerations are likely to be a more important factor than surface charge density in determining the ultimate amount of polymer adsorbed.

The pH-range requirement for maximal polymer coverage confirms that the mechanism of polymer adsorption depends on an electrostatic interaction between the surface and the polymer. At pH values lower than the isoelectric point of the surface, both the polymer and the surface are positively charged, and no electrostatically driven adsorption is expected to take place. At pH values higher than the pK_a of the polymer, the surface is negatively charged and the polymer is uncharged, and likewise, no electrostatically driven adsorption is expected to take place. However, at intermediate pH values, the polymer is positively charged and the surface is negatively charged, allowing for the electrostatically driven adsorption of the polymer onto the surface.

Experiments exploring the dependence of the PLL(375)-*g*[5.6]-PEG(5) adsorption behavior on the ionic strength of the

solution offer additional support to this adsorption model. Electrostatic shielding effects increase with increasing ionic strength, and therefore, electrostatically driven adsorption of polyelectrolytes, for example, is generally attenuated at high ionic strengths.

PLL(375)-g[5.6]-PEG(5) was also found to adsorb onto a preadsorbed layer of serum proteins. After a typical adsorption of serum protein (about 260 ng/cm²), subsequent exposure to a 1 mg/mL solution of PLL(375)-g[5.6]-PEG(5) led to an overlayer of polymer with a surface areal density of approximately 90 ng/cm². Earlier studies showed that the treatment of living red blood cells with PLL(375)-g[5.6]-PEG(5) prevented their subsequent agglutination.⁵¹ The observation of PLL(375)-g[5.6]-PEG(5) adsorption onto an adsorbed protein layer confirms the model proposed to explain this effect.

4.2. Reduction of Protein Adsorption. The protein-suppression performance of the adsorbed layer of copolymer was found to depend on the areal density of PEG that was immobilized on the surface, and this amount was found to be limited only by the spatial packing of the PEG side chains, regardless of the backbone length and grafting ratio. Approximate values for both the spacing and the radius of gyration of the PEG side chains are required in order to estimate the extent of packing at the surface. If one assumes that the side chains were arranged in a two-dimensional lattice at the surface, then the distance between each PEG side chain (L) (that is, the distance between each neighboring point within the lattice) can be calculated from the adsorbed copolymer areal density data. The radius of gyration (R_g) of the PEG side chains was estimated using an empirical equation based on static light-scattering measurements.⁵²

$$R_g = 0.181N^{0.58} \text{ (nm)} \quad (1)$$

where N is the number of repeat units. Such an estimate provides radii of gyration of about 1.65 and 2.82 nm for PEG side chains of mol wt 2000 and 5000, respectively. Calculated from the spacing (L) and the radius of gyration (R_g), the quantity $L/2R_g$ provides a value that represents the extent of packing on the surface. That is, values of $L/2R_g$ that are less than unity imply that the radii of gyration of neighboring PEG side chains overlap and that the surface is densely packed. Conversely, values of $L/2R_g$ that are greater than unity imply that there is space between neighboring PEG side chains, as their radii of gyration do not overlap.⁵³

The data presented in Figure 10 include protein-adsorption data from several different surface-immobilized PEG systems, including graft copolymers on metal oxide surfaces as described herein, self-assembled-monolayer-forming oligo(ethylene glycol) alkanethiolates⁵⁴ on gold surfaces, and poly(ethylene glycol) covalently bound to silanized silica.⁵³ Values from this work are compared to published data, for which both the areal mass density of proteins and the average PEG spacing (L) are taken from refs 53 and 54. The radii of gyration were calculated according to eq 1 for PEG, whereas the original value of 0.42 nm was used for the oligo(ethylene glycol). The evaluated data for the PLL-g-PEG graft copolymer system are in agreement with the evaluated data for the previously reported systems. The trend shown in Figure 10 suggests that the best protein-adsorption-suppression performance is observed for systems with the lowest $L/2R_g$ values and that, as $L/2R_g$ increases, the average spacing between the immobilized PEG chains increases and the suppression of protein adsorption decreases. Furthermore, the $L/2R_g$ value of 0.47 appears to be the limit of packing density, as $L/2R_g$ values lower than 0.47 were never observed

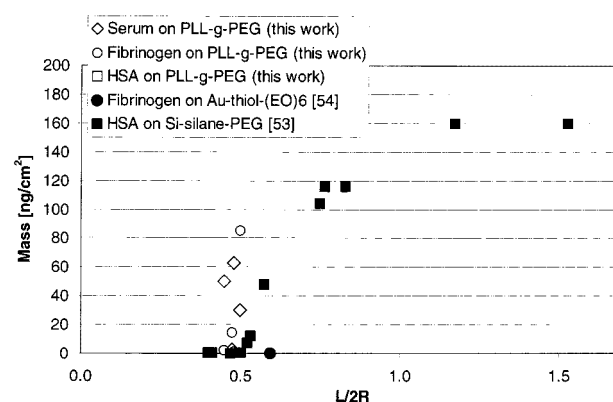


Figure 10. Dependence of serum adsorption on the extent of surface PEG side chain packing density. $L/2R_g$ is calculated as described in section 4.2. Values from this work are compared to published data, for which both the areal mass density of proteins and the average PEG spacing (L) are taken from refs 53 and 54. The radii of gyration were calculated according to eq 1 for PEG, whereas the original value of 0.42 nm was used for the oligo(ethylene glycol).

within our study and such values would imply an entropically unfavorable interaction between the PEG side chains.

The highest protein resistance among the PLL-g-PEG molecules investigated in this work was exhibited by PLL(20)-g[3.5]-PEG(2) and PLL(20)-g[5]-PEG(2), which often showed residual adsorbed masses of serum and fibrinogen, respectively, on the order of the detection limit of the OWLS technique (~ 2 ng/cm²). This is an important finding because it has been shown that there is a lower limit of fibrinogen adsorbed mass (~ 5 ng/cm²) below which the pathways leading to blood coagulation and thrombosis are not activated.⁵⁵

5. Conclusions

All of the copolymers discussed here, all of which were based on poly(L-lysine)-g-poly(ethylene glycol) (PLL-g-PEG), were found to adsorb spontaneously in an electrostatically driven process onto several different negatively charged metal oxide surfaces. The adsorption process was rapid and was ultimately limited by the packing of the PEG side chains at the surface. The resulting adsorbed layer was found to drastically reduce the subsequent interfacial protein adsorption. Reduction of protein adsorption was observed for all of the different PLL-g-PEG copolymer architectures investigated. However, only in the case of optimized PLL-g-PEG architectures could extremely low levels of serum and fibrinogen (on the order of < 5 ng/cm²) be achieved. In addition, antibody experiments gave evidence that the adsorbed serum mass that was observed was due not to proteins but rather to other components of the serum. The combination of data obtained from X-ray photoelectron spectroscopy and optical waveguide measurements suggests that the backbone of the copolymer acts as an anchor to the solid metal oxide surface, thereby exposing the PEG side chains to the solution phase and yielding a "comblake" interface configuration. Furthermore, the anchoring backbone of the copolymer appears to be capable of bridging surface contamination, still producing a protein-resistant surface. This observation and the fact that devices with complex shapes can be easily treated by PLL-g-PEG make the PLL-g-PEG surface-treatment technology a candidate for future applications in both the biomaterial/implant and biosensor areas. As a next step, proof-of-concept studies are envisioned to investigate the long-term performance of the polymer adlayers under more application-relevant conditions, such as contact with blood flow.

References and Notes

- (1) Leonard, E. F.; Turitto, V. T.; Vroman, L. *Blood in Contact with Natural and Artificial Surfaces*; New York Academy of Sciences: New York, 1987; Vol. 516.
- (2) Jeon, S. I.; Lee, J. H.; Andrade, J. D.; de Gennes, P. G. *J. Colloid Interface Sci.* **1991**, *142*, 149–166.
- (3) Isreals, R.; Leermakers, F. A. M.; Fleer, G. J. *Macromolecules* **1995**, *28*, 1626–1634.
- (4) Bjorling, M. *Macromolecules* **1992**, *25*, 3956–3970.
- (5) Claesson, P. *Colloids Surf., A* **1993**, *77*, 109–118.
- (6) Gombotz, W. R. *Surfaces: Synthesis, Characterization and Biological Interaction Studies*; University of Washington: Seattle, WA, 1988.
- (7) Gombotz, W. R.; Guanghui, W.; Hoffman, A. S. *J. Appl. Polym. Sci.* **1989**, *37*, 91–107.
- (8) Schroen, C. G. P. H.; Stuart, M. A. C.; van der Voort Maarschaalk, K.; van der Padt, A.; van't Riet, K. *Langmuir* **1995**, *11*, 3068–3074.
- (9) Freij-Larsson, C.; Nylander, T.; Jannasch, P.; Wesslen, B. *Biomaterials* **1996**, *17*, 2199–2207.
- (10) Amiji, M. M.; Park, K. *J. Appl. Polym. Sci.* **1994**, *52*, 539–544.
- (11) Amiji, M.; Park, K. *Biomaterials* **1992**, *13*, 682–692.
- (12) Lee, J. H.; Kopeckova, P.; Kopecek, J.; Andrade, J. D. *Biomaterials* **1990**, *11*, 455–464.
- (13) Lee, J. H.; Kopecek, J.; Andrade, J. D. *J. Biomed. Mater. Res.* **1989**, *23*, 351–368.
- (14) Balazs, A. C.; Siemasko, C. P. *J. Chem. Phys.* **1991**, *95*, 3798–3803.
- (15) van der Linden, C. C.; Leermakers, F. A. M.; Fleer, G. J. *Macromolecules* **1996**, *29*, 1000–1005.
- (16) Kosmas, M. K. *Macromolecules* **1990**, *23*, 2061–2065.
- (17) Marzio, E. A. D.; Gutmann, C. M.; Mah, A. *Macromolecules* **1995**, *28*, 2930–2937.
- (18) Marques, C. M.; Joanny, J. F. *Macromolecules* **1990**, *23*, 268–276.
- (19) Halperin, A.; Tirrell, M.; Lodge, T. P. *Adv. Polym. Sci.* **1992**, *100*, 31–71.
- (20) Kawaguchi, M.; Takahashi, A. *J. Colloid Interface Sci.* **1992**, *37*, 219–317.
- (21) Hoogeveen, N. G.; Stuart, M. A. C.; Fleer, G. J. *Faraday Discuss.* **1994**, *98*, 161–172.
- (22) Hoogeveen, N. G.; Stuart, M. A. C.; Fleer, G. J. *J. Colloid Interface Sci.* **1996**, *182*, 146–157.
- (23) Hoogeveen, N. G.; Stuart, M. A. C.; Fleer, G. J. *J. Colloid Interface Sci.* **1996**, *182*, 133–145.
- (24) Hubbell, J. A.; Sawhney, A. S. Biocompatible Microcapsules. U.S. Patent 5,232,984, 1993.
- (25) Hubbell, J. A.; Elbert, D. L.; Hill-West, J. L.; Drumheller, P. D.; Chowdhury, S.; Sawhney, A. S. Multifunctional Organic Polymers. U.S. Patent 5,462,990, 1995.
- (26) Hubbell, J. A.; Sawhney, A. S. Biocompatible Microcapsules. U.S. Patent 5,380,536, 1995.
- (27) Hubbell, J. A.; Donald, D. L. E.; Hill-West, J. L.; Drumheller, P. D.; Chowdhury, S.; Sawhney, A. S. Methods for Modifying Cell Contact with a Surface. U.S. Patent 5,567,440, 1996.
- (28) Choksakulnimitr, S.; Musada, S.; Tokuda, H.; Takakura, Y.; Hashida, M. *J. Controlled Release* **1995**, *34*, 233–241.
- (29) Clegg, J. A.; Hudecz, F.; Mezo, G.; Pimm, M. V.; Szekerke, M.; Baldwin, R. W. *Bioconjugate Chem.* **1990**, *1*, 425–430.
- (30) Ryser, H. J. P.; Mandel, R.; Hacopian, A.; Chen, W. *J. Cell. Physiol.* **1988**, *135*, 277–284.
- (31) Koyo, H.; Tsuruta, T.; Kataoka, K. *Polym. J.* **1993**, *25*, 141–152.
- (32) Bogdanov, A. A.; Martin, C.; Bogdanova, A. V.; Brady, T. J.; Weissleder, R. *Bioconjugate Chem.* **1996**, *7*, 144–149.
- (33) Bogdanov, A. A.; Weissleder, R.; Frank, H. W.; Bogdanova, A. V.; Nossif, N.; Schaffer, B.; Tsai, E.; Papisov, M. I.; Brady, T. J. *Radiology* **1993**, *187*, 701–706.
- (34) Elbert, D. L.; Hubbell, J. A. *J. Biomed. Mater. Res.* **1998**, *42*, 55–65.
- (35) Ramsden, J. J. *J. Stat. Phys.* **1993**, *73*, 853–877.
- (36) Kurrat, R.; Textor, M.; Ramsden, J. J.; Boni, P.; Spencer, N. D. *Rev. Sci. Instrum.* **1997**, *68*, 2172–2176.
- (37) Kurrat, R.; Walivaara, B.; Marti, A.; Textor, M.; Tengvall, P.; Ramsden, J. J.; Spencer, N. D. *Colloids Surf.* **1998**, *11*, 187–201.
- (38) Ramsden, J. J.; Mate, M. *J. Chem. Soc., Faraday Trans.* **1998**, *94*, 783–788.
- (39) Jukubauskas, H. L. *J. Coat. Technol.* **1986**, *58*, 71–82.
- (40) Xu, R.; D'Unger, G.; Winnik, M. A.; Marinho, J. M. G.; d'Oliviera, J. M. R. *Langmuir* **1994**, *10*, 2977–2984.
- (41) Tripp, C. P.; Hair, M. L. *Langmuir* **1996**, *12*, 2.
- (42) Pefferkorn, E.; Elaissari, A.; Huguenard, C. *Macromol. Rep.* **1992**, *A29*, 147–153.
- (43) Tirrell, M.; Parsonage, E.; Watanabe, H.; Dhoot, S. *Polym. J.* **1991**, *23*, 641–664.
- (44) Stuart, M. A. C.; Fleer, G. J.; Lyklema, J.; Norde, W. *Adv. Colloid Interface Sci.* **1991**, *34*, 477–535.
- (45) Kurrat, R. Adsorption of Biomolecules on Titanium Oxide Layers in Biological Model Solutions. Ph.D. Dissertation, ETH Zurich, Zurich, Switzerland, 1998.
- (46) Ramsden, J. J.; Roush, D. J.; Gill, D. S.; Kurrat, R.; Willson, R. C. *J. Am. Chem. Soc.* **1995**, *117*, 8511–8516.
- (47) Moulder, J. F.; Stickle, W. F.; Sobol, P. E.; Bomben, K. D. *Handbook of X-ray Photoelectron Spectroscopy*; Perkin-Elmer Corp.: Eden Prairie, MN, 1992.
- (48) Marti, A. Untersuchung Lokaler Chemischer und Tribologischer Eigenschaften von Oxidischen und Organischen Oberflaechen in Elektrolytloesung mit dem Raterkraftmikroskop. Ph.D. Dissertation, ETH Zurich, Zurich, Switzerland, 1997.
- (49) Healy, T. W.; White, L. R. *Adv. Colloid Interface Sci.* **1978**, *9*, 304–345.
- (50) Vörös, J.; Höök, F.; Askendal, A.; Wälivaara, B.; Tengvall, P.; Kasemo, B.; Ramsden, J. J.; Böni, P.; Kurrat, R.; Textor, M.; Spencer, N. D. *Colloids Surf.* **1999**, submitted for publication.
- (51) Elbert, D. L.; Hubbell, J. A. *Chem. Biol.* **1998**, *5*, 177–183.
- (52) Kawaguchi, S.; Imai, G.; Suzuki, J.; Miyahara, A.; Kitano, T. *Polymer* **1997**, *38*, 2885–2891.
- (53) Sofia, S. J.; Premnath, V.; Merrill, E. W. *Macromolecules* **1998**, *31*, 5059–5070.
- (54) Harder, P.; Grunze, M.; Dahint, R.; Whitesides, G. M.; Laibinis, P. E. *J. Phys. Chem. B* **1998**, *102*, 426–436.
- (55) Tsai, W. B.; Grunkemeier, J. M.; McFarland, C. D.; Horbett, T. A. *Selectively Depleted Plasmas To Study the Role of Four Plasma Proteins in Platelet Adhesion to Biomaterials*; LeBerge, M., Agrawal, C. M., Eds.; Society for Biomaterials: Providence, RI, 1999; Vol. 22, p 266.